Nanodispersed Platinum on Chemically Treated Nanostructured Carbonized Polyaniline as a New PEMFC Catalysts

Nemanja M. Gavrilov[1], Igor A. Pašti[1], Gordana Ćirić-Marjanović[1], Vladimir M. Nikolić[2], Milica P. Marčeta Kaninski[2], Šćepan S. Miljanić[1,2], Slavko V. Mentus[1,3,]*

[1] University of Belgrade, Faculty of Physical Chemistry, Studentski trg 12-16, 11158 Belgrade, Serbia
[2] University of Belgrade, Vinča Institute for Nuclear Sciences, Mike Petrovića Alasa 12-14, 11001 Vinča, Serbia
[3] Serbian Academy of Science and Arts, Knez Mihajlova 35, 11000 Belgrade, Serbia
[*]E-mail: slavko@ffh.bg.ac.rs

The surface of nitrogen containing carbonized nanostructured polyaniline (Carb-nanoPANI) was modified by a chemical treatment with NaOH, H_2O_2 and HNO_3 at room temperature. The modification was controlled by FTIR and Raman spectroscopies. The modified materials were used as an unconventional support of nanodispersed platinum electrocatalysts, built in further in a polymer electrolyte membrane fuel cell (PEMFC). The surface treatment influenced the mean platinum particle diameter, and consequently, the performance of PEMFC too. In comparison to a conventional nanodispersed Pt/C catalyst in the same cell, these electrocatalysts provided up to 34% higher power density. Apart of surface modification, a particular chemical composition of Carb-nanoPANI support itself was suggested to be responsible for the observed PEMFC performance improvement.

Keywords: carbonized polyaniline, catalysts support, chemical treatment, PEMFC, platinum electrocatalysts

1. INTRODUCTION

Platinum is known as the best elemental catalyst for electrode reactions such as oxygen reduction reaction (ORR) and ethanol oxidation in fuel cells. Much research effort was invested to enhance its catalytic effectiveness. The literature reports describe the attempts to reduce platinum content in the catalyst, either by making platinum alloys with more abundant metals [1-3], or by

enlarging the real catalyst surface area by means of a large surface area support [4]. As the carriers/supports enabling high dispersion of precious metal, different types of nanodispersed carbon were used, such as carbon nanofibers [5,6], carbon nanotubes (CNT) [7] including nitrogen containing carbon nanotubes (NCNT) [8], etc. As overviewed by Qiao and Li [9], the size, shape and dispersion uniformity of Pt nanoparticles (PtNPs) on supporting materials play a crucial role in their catalytic activity. The maximum mass activity of supported PtNPs toward ORR was achieved with Pt particles 3–4 nm in diameter. Such a mean particle size offered also the highest durability of catalyst performance [9]. Acid/oxidative treatment of carbonaceous nanostructures was found to introduce various oxygen-containing surface functional groups and was recognized to be very helpful in obtaining high catalyst dispersion [10]. In spite of the fact that this type of treatment offers versatility, efficiency and potential to scale-up, a relationship between the amounts of O-containing surface functional groups in the carbon support and the amount of anchored metal is still under a debate [10]. The most common reagents used for liquid-phase oxidation treatment are HNO_3, H_2SO_4, and H_2O_2 [10,11].

In contrast to commonly reported procedures for preparing NCNT, such as nanotube growing on a metal-catalysed substrate, thermal chemical vapor deposition or nitriding of pure nanostructured carbon under nitrogen containing gases and vapors, carbonization of N-containing nanostructured polymers such as polyaniline (PANI) was recognized as a simple and efficient new route to various types of N-containing carbon nanostructures [12–16] generally very rich in nitrogen, close to 10 %. The carbonization of PANI nanotubes has especially been pointed out as a promising route for an industrial-scale preparation of NCNT [12,14,17]. Mentus et al. [12] recently reported preparation of carbonized PANI nanotubes which had a typical outer diameter of 100–260 nm, with an inner diameter of 20–170 nm and a length extending from 0.5 to 0.8 μm, accompanied with very thin nanotubes with outer diameters of 8–14 nm, inner diameters 3.0–4.5 nm and length extending from 0.3 to 1.0 μm. Conductivity of carbonization products of nanotubular PANI amounted to 0.7 S cm^{-1}. Carbonized PANI nanostructures (Carb-nanoPANI) have been proposed as a chemically inert and a thermally stable support for the deposition of noble-metal catalyst [18], while the usability of Carb-nanoPANI as PtNPs catalyst support for ORR and ethanol electro-oxidation catalysts was recently demonstrated for the first time by our group [19].

The aim of this work is to demonstrate the effects of chemical treatment in NaOH, H_2O_2 and HNO_3 solutions of N-containing carbon nanomaterial, designed as Carb-nanoPANI, on the mean platinum particle dimension upon platinum deposition from an aqueous solution. The variances of the obtained Pt-based nanodisperzed electrocatalysts, designated generally as PtNPs/Carb-nanoPANI, were evaluated as cathode catalyst in a proton exchange membrane fuel cell (PEMFC). The origin of PEMFC performance improvement achieved upon chemical surface treatment of carbon material was discussed in view of the functional groups introduced on Carb-nanoPANI surface.

2. EXPERIMENTAL

2.1. Catalyst synthesis

Conducting Carb-nanoPANI was synthesized as described elsewhere [12,16]. Its chemical pretreatment was carried out in 3M HNO_3, 30% H_2O_2 and 1 M NaOH solution under ultrasonication for 6 h. The samples are further denoted as Carb-nanoPANI-(chemical agent). The PtNPs were deposited by a modified polyol method [19,20]. Shortly, Carb-nanoPANI was dispersed in ethylene glycole (EG) and the hexachloroplatinic acid/EG solution was added drop wise under agitation by a magnetic stirrer. The pH value was adjusted to 10 by NaOH/EG solution. The homogeneous slurry was then heated at 120 °C for 2 h to evaporate the solvent. Upon cooling to room temperature, the material was filtered, washed with ethanol and distilled water and dried. The resulting fine black powder was subjected to heating at 300 °C for 2 h under H_2/Ar stream to obtain PtNPs/Carb-nanoPANI. The ratio of platinum metal against dry Carb-nanoPANI in the starting slurry was 20%.

2.2. Support and catalyst characterization

Raman spectra excited with a diode-pumped solid state laser (excitation wavelength 532 nm) were collected on a DXR Raman microscope (Thermo Scientific). Infrared spectra of the powdered samples dispersed in KBr pellets were recorded in the range of 400–4000 cm^{-1} using a Nicolet 6700 FTIR Spectrometer (Thermo Scientific). The mass fraction of Pt was checked within TA SDT 2960 thermobalance, by combusting the carbon support under an air stream, at a flow rate of 50 cm^3 min^{-1} and a heating rate of 10 °C min^{-1}. The X-ray powder diffraction (XRPD) patterns were obtained on a Philips PW-1710 automated diffractometer using Cu tube ($\lambda = 1.5418$ Å) operated at 40 kV and 30 mA. Diffraction data were collected in the range of $2\theta = 35$–$75°$, by a step size of $0.05°$ and a counting time of 7.20 s per step.

2.3. Preparation of membrane electrode assembly and fuel cell testing procedure

2.3.1. Preparation of electrodes

The electrodes for fuel cells were prepared using AvCarb ™ P75T carbon paper for gas diffusion layer (GDL). The GDL is formed by brushing 1.25% polytetrafluoroethylene (PTFE) solution on 5 cm^2 carbon paper and sintered for one hour at 360°C in N_2 atmosphere. The amount of PtNPs/Carb-nanoPANI used was adjusted to yield the platinum loading of 0.4 mg cm^{-2} and 0.2 mg cm^{-2}, for cathode and anode, respectively. For comparison purposes, commercial 40% Pt/C catalyst (Alfa Aesar, HiSPECTM 4000, product no. 42204, average particle size 3.9 nm [21]) was used. In this case, the platinum loading was adjusted to amount to 0.8 mg cm^{-2} on both cathode and anode. With the mentioned Pt loadings, an identical total catalyst (Pt + support) loading at the cathode, i.e. 2 mg cm^{-2}, was obtained. In this way, the thickness of the catalyst layer was kept constant, enabling a mutual comparability of the results obtained with various catalysts. By multiple measurements, the repeatability of the results was confirmed.

2.3.2. Preparation of membrane electrode assembly (MEA)

The membrane Nafion 117 (DuPont) was boiled in 5% H_2O_2 for one hour, to remove any organic impurities, then in 10% H_2SO_4 for an hour, to eliminate surely any metallic impurities, as well as to convert the membrane completely to a H^+ form [22]. Finally, it was boiled in distilled water for an hour. The MEA was prepared by hot pressing of Nafion membrane sandwiched between the cathode and the anode at 120° C for 10 min.

2.3.3. Current–voltage characteristics

The MEA was inserted into Arbin fuel cell hardware and connected to the test station (HepasMini150) equipped with a gas humidifier, a mass flow controller, and a temperature indicator controller. Assembled fuel cell was fed with oxygen (cathode) and hydrogen (anode) gas stream at flow rate of 0.3 l/min and 0.6 l/min, respectively. Current – voltage (I-V) characteristics were measured under the following conditions: cell temperature: 80^oC, relative humidity: 100 %, kept by means of electronic load station HephasMini150.

3. RESULTS AND DISCUSSION

3.1. Effects of chemical treatment on the molecular structure of Carb-nanoPANI catalyst support
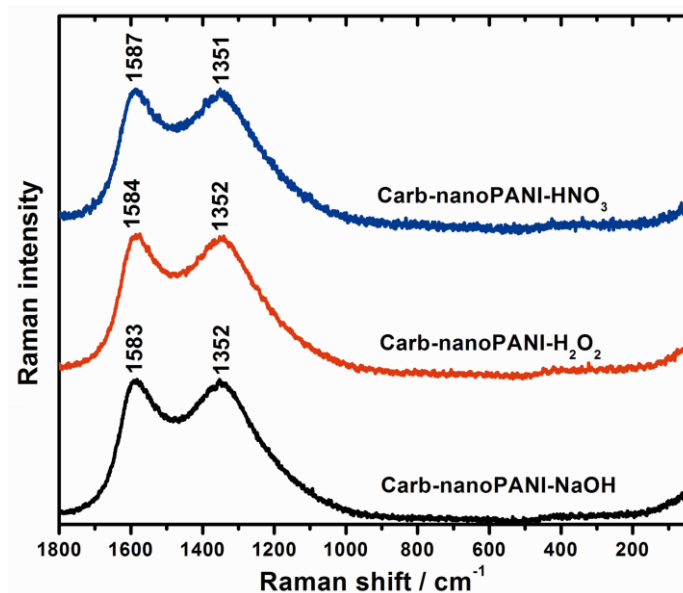

Figure 1. Raman spectra of Carb-nanoPANI treated with NaOH, H_2O_2, and HNO_3.

The Raman spectra of investigated chemically treated Carb-nanoPANI (Fig. 1) show two main broad bands with maxima at ~1585 cm^{-1} (graphite-like G-band) and 1352 cm^{-1} (D-band, labeled "D" for the disordered form), characteristic for disordered graphites [12,18,23]. The peak intensity ratio

I_D/I_G, determined using integrated peak areas, was evaluated to be 3.24, 3.21 and 3.29 for Carb-nanoPANI-NaOH, Carb-nanoPANI-H$_2$O$_2$ and Carb-nanoPANI-HNO$_3$, respectively. As the D band reflects the presence of disorder in sp^2-hybridized carbon systems, obtained I_D/I_G values indicate significant disorder in all investigated samples, which is mainly due to the covalent incorporation of nitrogen and oxygen in the carbon sp^2 network structure. Since for untreated Carb-nanoPANI the ratio I_D/I_G was previously reported to be 3.48 [23], the new value of this ratio obtained upon chemical treatment means a degree of bond reorganization, i.e., a change of Carb-nanoPANI molecular structure.

The FTIR spectrum (Fig. 2) of Carb-nanoPANI-NaOH sample consists of two main broad bands with the maxima at 1576 and 1261 cm^{-1}, corresponding to the G-band and the D-band, respectively [12,18]. The band at 1576 cm^{-1} was attributed to C=N stretching modes mixed with aromatic C–C stretching vibrations [12,24], while the band at 1261 cm^{-1} was attributed to the vibrations of various C–N and C–C bonds [12,18]. FTIR spectrum of Carb-nanoPANI-NaOH sample was found to be the same as the FTIR spectrum of non-treated Carb-nanoPANI [12,23], indicating that NaOH treatment does not induce any significant changes in the surface composition of this material. FTIR spectra of Carb-nanoPANI-H$_2$O$_2$ and Carb-nanoPANI-HNO$_3$ (Fig. 2) differ from the spectrum of Carb-nanoPANI-NaOH sample in two aspects: by the appearance of a new very sharp band at 1384 cm^{-1}, and by a shift of G-band towards the higher wavenumbers, from 1589 cm^{-1}, for Carb-nanoPANI-H$_2$O$_2$, to 1594 cm^{-1}, for Carb-nanoPANI-HNO$_3$, the later being much stronger. The band at 1594 cm^{-1} can be assigned to the N$^+$–O$^-$ stretching vibration in N-oxide structural units, to the symmetric stretching vibration of nitro group, and to the vibration of nitrate anion [25,26] (Fig. 2).
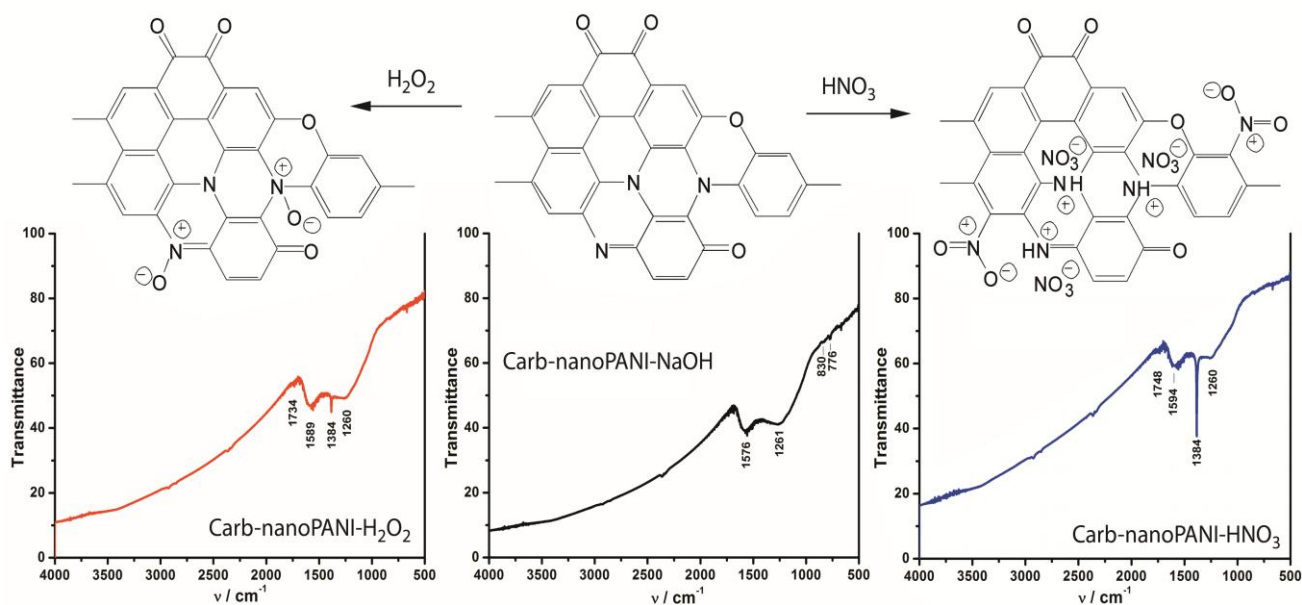

Figure 2. The scheme of the reactions on the Carb-nanoPANI surface: formation of N$^+$–O$^-$ bonds in H$_2$O$_2$ solution, and nitration and protonation in HNO$_3$ solution, together with the corresponding FTIR spectra of Carb-nanoPANI recorded upon the chemical treatment.

The weak peaks at 1734 and 1748 cm^{-1} in the FTIR spectra of Carb-nanoPANI-H$_2$O$_2$ and Carb-nanoPANI-HNO$_3$, respectively, can be attributed to the stretching of C=O group. A broad absorption over the whole range 4000 - 500 cm^{-1} is observed in the FTIR spectra of all samples, assigned to the excitation of free conducting electrons [18]. Obtained results confirm unambiguously an incorporation of new surface functionalities obtained through the oxidation of nitrogen surface functional groups of starting material, in the case of H$_2$O$_2$ treatment, and through the nitration of aromatic rings as well as through the protonation of basic nitrogen atoms of starting Carb-nanoPANI, in the case of HNO$_3$ treatment.

### 3.2. Electrocatalyst characterization and PEMFC performance

The alteration of surface functional groups of Carb-nanoPANI is expected to affect the number and the distribution of nuclei of PtNPs and their surface adhesion, during the synthesis of PtNPs/Carb-nanoPANI electrocatalysts. The TGA analysis revealed no losses of Pt during the synthesis and confirmed the weight fraction of Pt to be 20% in each of the electrocatalysts. On the other hand, XRPD patterns (Fig. 3) revealed different size of PtNPs depending on the particular chemical treatment.

The smallest particles with an average diameter of 5.1 nm were evidenced in the case of PtNPs/Carb-nanoPANI-HNO$_3$ electrocatalyst, while the largest particles (8.3 nm) were observed in the case of PtNPs/Carb-nanoPANI-NaOH electrocatalyst. In the case of PtNPs/Carb-nanoPANI-H$_2$O$_2$ electrocatalyst average particle size was found to be 5.5 nm.
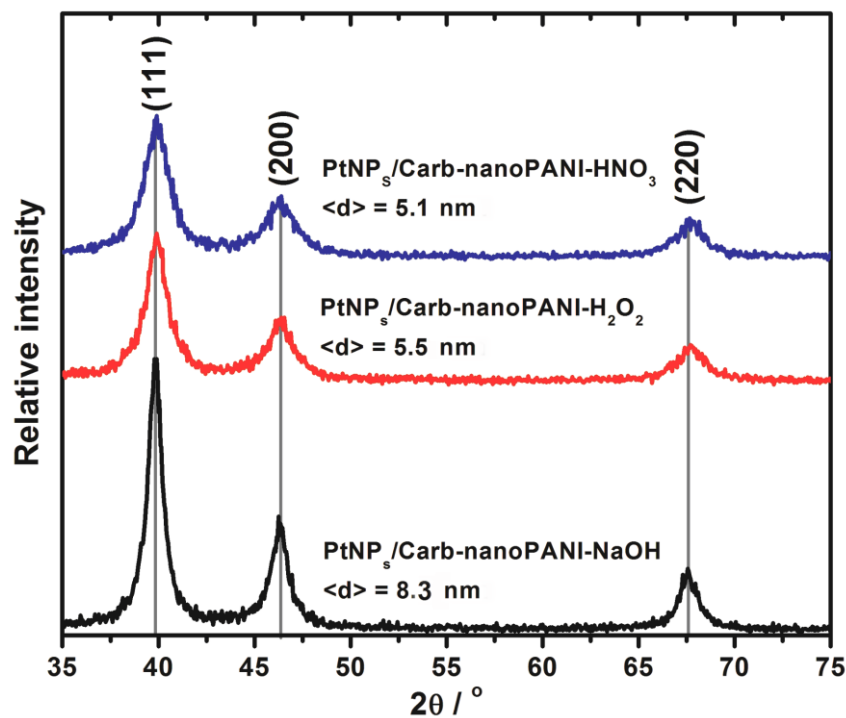
Figure 3. XRPD patterns of synthesized PtNPs/Carb-nanoPANI electrocatalysts (average particle diameters (<d>) were calculated by means of the Scherrer equation).

The size of Pt particle can be correlated with the surface functionalization, as evidenced from the FTIR spectra of chemically treated Carb-nanoPANI supports.
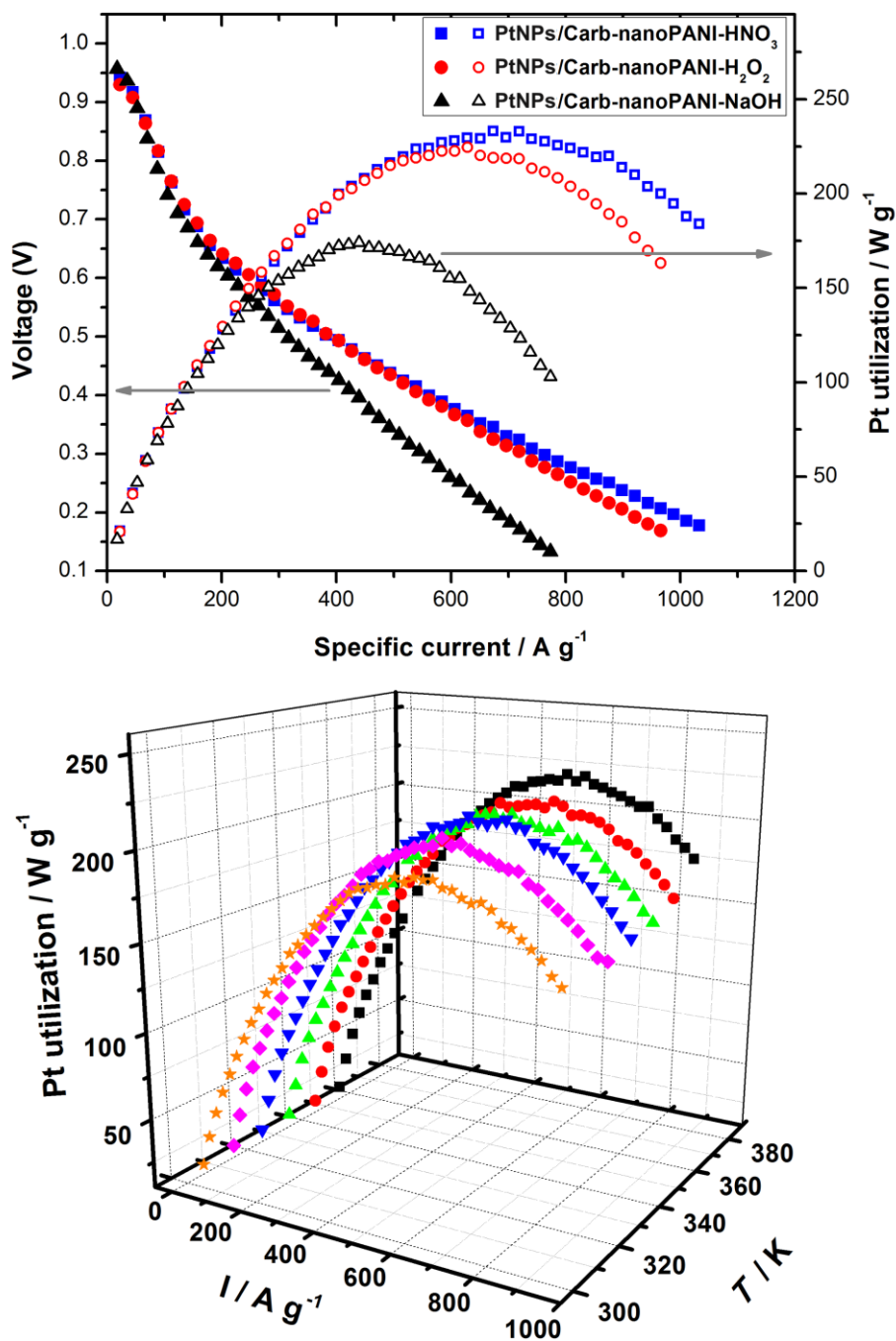
Figure 4. top: Platinum utilization expressed as specific power (W g^{-1}), and voltage in function of current density (in A g^{-1}), for three single PEM fuel cells with PtNPs/Carb-nanoPANI catalysts at T = 353 K; down: 3D presentation of platinum utilization in function of current density, at different temperatures, for PtNPs/Carb-nanoPANI- HNO$_3$ cathode.

FTIR and XPRD results indicate that new N-oxide (N^+-O^-) and nitro groups, accompanied with nitrate anions, introduced by Carb-nanoPANI treatment with H_2O_2 and HNO_3, respectively, serve as an additional anchoring sites for Pt nucleation in the course of the synthesis, resulting in higher dispersion of platinum over Carb-nanoPANI supports. The dispersion of Pt over the Carb-nanoPANI supports, tuned by pre-synthetic chemical treatment, was further confirmed to have significant role in PEMFC performance. It is important to emphasize that Carb-nano-PANI does not display any significant ORR activity in acidic media, serving well as an inert catalyst support, while in alkaline solution it offers both an appreciable ORR catalytic activity and an ability of further improvement of ORR activity by a simple post-synthetic treatment [23].

The data obtained (Fig. 4, top) show that the Pt utilization, expressed through power density output at different currents, achieves the maximum for the fuel cell with the PtNPs/Carb-nanoPANI-HNO_3 catalyst operating as the cathode catalyst. For the same electrocatalyst, the dependence of Pt utilization at different currents on the operating temperature is provided too (Fig. 4, bottom). The best performance of PtNPs/Carb-nanoPANI-HNO_3 as the cathode catalyst is obtained with the smallest Pt particle size, i.e. the largest surface area. The commercial Pt/C catalyst was tested in the same cell using the same overall loading, providing maximum Pt utilization of 174 W g^{-1}. Comparing the PEMFC performance obtained by use of new PtNPs/Carb-nanoPANI electrocatalysts, to the ones obtained by use of commercial Pt/C electrocatalyst, one may see generally that higher Pt utilization was achieved by means of new PtNPs/Carb-nanoPANI electrocatalysts.

The PtNPs/Carb-nanoPANI-HNO_3 electrocatalysts gave Pt utilization amounting to 233 W g^{-1}, when calculated with respect to the cathode Pt loading. In comparison to the commercial Pt/C catalyst, this presents a 34 % higher Pt utilization. These results sound with the previously published ones related to the application of some other unconventional PtNPs supports for PEMFC application. For instance, Shao et al. [27], for multi-walled CNTs as PtNPs support, reported currents densities between 35 and 60 A g^{-1} at 0.6 V, depending on the pre-synthetic treatment of support. The Pt loading reported amounted to 0.29 mg cm^{-2}, while the mean particle diameter ranged from 2.5 to 4 nm. One can see from Fig. 4 that the application of Carb-nanoPANI support is beneficial. However, one should keep in mind that the observed PEMFC performance is highly dependent not only on the intrinsic activity of catalysts, but also on some other factors.

One more important conclusion relating to the enhancement of Pt utilization by means of chemically treated PtNPs/Carb-nanoPANI catalysts is made comparing the specific surface area of Pt in these and commercial catalysts. Namely, commercial Pt/C catalyst has smaller Pt particles, providing higher Pt specific surface area, S_{Pt}, compared to any PtNPs/Carb-nanoPANI catalysts. The specific surface area (in units m^2 g^{-1}) can be easily estimated using the equation $S_{Pt} = 6000/(<d>\cdot\rho)$, where $<d>$ and ρ are average particle size in nm and Pt density (21.45 g cm^{-2}), respectively. For the PtNPs/Carb-nanoPANI catalysts, S_{Pt} was estimated to amount to 34, 51 and 54 m^2 g^{-1} upon chemical treatment with NaOH, H_2O_2 and HNO_3, respectively, while for commercial Pt/C used in this study, S_{Pt} amounted to 72 m^2 g^{-1}, with the particles size in the optimal diameter range for ORR [9]. Taking into account the Pt loading of the cathode, commercial Pt/C catalysts disposed with 4.2 times higher Pt surface per square centimeter of cathode, relative to the PtNPs/Carb-nanoPANI-NaOH catalyst. Regardless of the fact that PtNPs/Carb-nanoPANI-NaOH, among the three PtNPs/Carb-nanoPANI

catalyst studied, had the lowest Pt specific surface area (34 m^2 g^{-1}), its Pt utilization in PEMFC was not lower than the one of commercial Pt/C catalyst with S_{Pt} =72 m^2 g^{-1} and even double loading. Neglecting in this consideration the possible small negative effect of loading on Pt utilization (Taylor et al. [28] evidenced that 10-fold increase of Pt loading reduces Pt utilization by 50%), we may conclude that PtNPs/Carb-nanoPANI display largely higher catalyst effectiveness per unit mass of Pt relative to the commercial Pt/C catalyst.

The gain in catalyst activity in the case of PtNPs/Carb-nanoPANI catalysts may be attributed to the recently confirmed intrinsic electrocatalytic activity of very Carb-nanoPANI materials toward ORR [14,15,23]. Therefore, it would be of great importance to provide an insight in the role of N-dopant in the PtNPs/Carb-nanoPANI catalyst system. As overviewed by Zhou et al. [29], there are three modes of action of N-dopant: i) alteration of catalyst nucleation and growth behavior, ii) N-dopant induced alteration of binding of noble phase with support (anchoring) and iii) alteration of electronic structure and reactivity. In our previous report [19] high electrocatalytic activity of PtNPs/Carb-nanoPANI-NaOH towards ORR was demonstrated, proving beneficial presence of N-dopant in catalyst support, which might be attributed to the increased intrinsic activity achieved through altered electronic structure of deposited PtNPs. On the other hand, oxidation of surface nitrogen functionalities resulted in further improved dispersion of Pt nanoparticles over Carb-nanoPANI support, reflecting the PEMFC performance. However, in this specific case there are no evidences that modification of nitrogen surface functionalities (Fig. 2) induces any further change of Pt electronic structure and reactivity. This conclusion is supported by a direct linear correlation of Pt utilization and Pt specific surface area (Fig. 5).
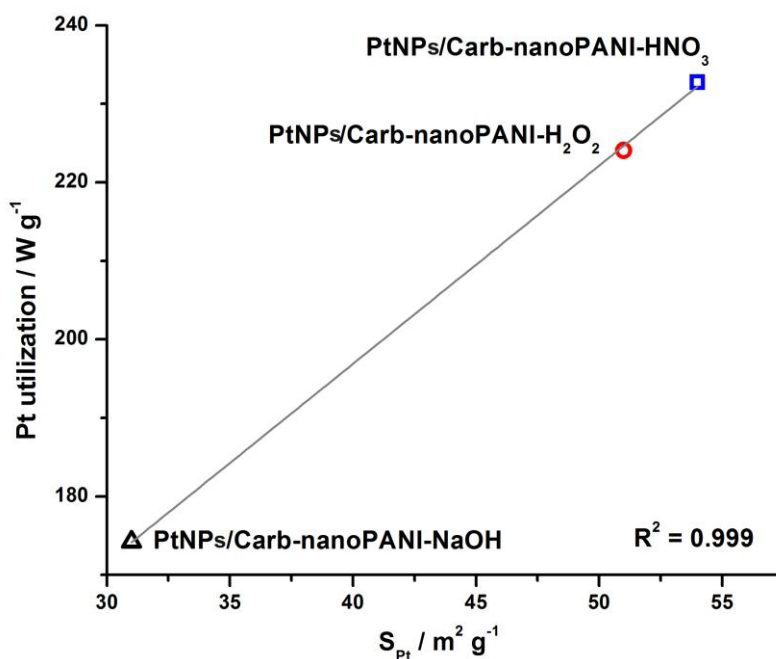
Figure 5. Pt utilization, *vs.* specific surface area of Pt estimated by means of the equation $S_{Pt} = 6000/(\langle d \rangle \cdot \rho)$, where $\langle d \rangle$ and ρ are average particle size in nm and Pt density (21.45 g cm^{-2}), respectively. The straight line presents the result of the best linear fit.

We suggest that any effect of newly introduced surface functionalities regarding modification of electronic structure of PtNPs would result in deviation from this linearity.

4. CONCLUSIONS

Conducting carbonized nanostructured PANI, entitled Carb-nanoPANI, upon chemical treatment by NaOH, H_2O_2 or HNO_3 was used as a nitrogen-containing carbon support for PtNPs PEMFC cathode electrocatalyst. By the FTIR spectroscopy the formation of new N-oxide (N^+–O^-) and nitro groups on Carb-nanoPANI surface was evidenced as a consequence of the treatment with H_2O_2 and HNO_3, respectively, while these groups were absent in Carb-nanoPANI samples treated with NaOH. The introduction of new N/O-containing surface functional groups, proposed to serve as additional anchorage sites, yielded a tuning effect on the size of PtNPs during their deposition, and consequently, on the PEMFC performance. The treatment of Carb-nanoPANI with HNO_3, enabled to obtain the smallest Pt nanoparticles (5.1 nm), and the best PEMFC performance. These results indicate the direct linking between PEMFC performance and the effectiveness of Carb-nanoPANI support in dispersing PtNPs, tuned by the surface modification. In addition, relative to the commercial Pt/C catalyst, an improvement of Pt utilization was evidenced for each of the observed PtNPs/Carb-nanoPANI catalysts. This general positive effect was attributed to activity of the Carb-nanoPANI support itself.

Large number of possible PANI nanostructures, able to be converted to nitrogen-containing nanostructured carbons, offers a vast number of possible new catalyst supports. The here demonstrated effects of chemical treatment of Carb-nanoPANI, having in mind their low cost and simple industrial production, open new perspectives in development of highly efficient Carb-nanoPANI–supported PEMFC electrocatalysts.

References

1. V. Stamenkovic, B. Fowler, B. Mun, G. Wang, P. Ross, C. Lucas and N. Markovic, *Science*, 315 (2007) 493.
2. W. Martínez M., T. Toledano Thompson, Mascha A. Smit, Int. J. Electrochem. Sci., 5 (2010) 931 – 943.
3. S. Rivas, L. G. Arriaga, L. Morales, A. M. Fernández, Int. J. Electrochem. Sci., 7 (2012) 3601 – 3609.
4. K. Chan, J. Ding, J. Ren, S. Cheng and K. Tsang, *J. Mater. Chem.*, 14 (2004) 505.

5. F. Alcaide, G. Álvarez, O. Miguel, M. Jesús Lázaro, R. Moliner, A. López-Cudero, J. Solla-Gullón, E. Herrero, A. Aldaz, Electrochem. Commun., 11 (2009) 1081-1084.
6. D. Sebastián, A. García Ruíz, I. Suelves, R. Moliner, M. Jesús Lázaro, V. Baglio, A. Stassi, A. Salvatore Aricò, Appl. Catal. B, 115-116 (2012) 269-275.
7. J. P. Singh, X. G. Zhang, Hu -lin Li, A. Singh and R.N. Singh, Int. J. Electrochem. Sci., 3 (2008) 416 – 426.
8. T. Maiyalagan, B. Viswanathan and U. Varadaraju, *Electrochem. Commun.*, 7 (2005) 905.
9. Y. Qiao and C. Li, *J. Mater. Chem.*, 21 (2011) 4027.
10. M. Carmo, M. Linardi and J. Poco, *Int. J. Hydrogen Energy*, 33 (2008) 6289.
11. Z. Špitalsky, C. Krontiras, S. Georga and C. Galiotis, *Composites Part A*, 40 (2009) 778.
12. S. Mentus, G. Ćirić-Marjanović, M. Trchová and J. Stejskal, *Nanotechnology*, 20 (2009) 245601.
13. C. Jin, T. Nagaiah, W. Xia, B. Spliethoff, S. Wang, M. Bron, W. Schuhmann and M. Muhler, *NanoScale*, 2 (2010) 981.
14. A. Janošević, I. Pašti, N. Gavrilov, S. Mentus, G. Ćirić-Marjanović, J. Krstić, J. Stejskal, *Synth. Met.*, 161 (2011) 2179.
15. A. Janošević, I. Pašti, N. Gavrilov, S. Mentus, J. Krstić, M. Mitrić, J. Travas-Sejdic, G. Ćirić-Marjanović, *Micropor. Mesopor. Mater.*, 152 (2012) 50.
16. N. Gavrilov, I. A. Pašti, M. Vujković, J. Travas-Sejdic, G. Ćirić-Marjanović, S. V. Mentus, *Carbon*, 50 (2012) 3915.
17. G. Ćirić-Marjanović, *Polyaniline Nanostructures. In: A. Eftekhari, ed., Nanostructured Conductive Polymers*, Wiley, London (2010).
18. M. Trchová, E. Konyushenko, J. Stejskal, J. Kovářová and G. Ćirić-Marjanović, *Polym. Degrad. Stab.*, 94 (2009) 929.
19. N. Gavrilov, M. Dašić-Tomić, I. Pašti, G. Ćirić-Marjanović and S. Mentus, *Mater. Lett.*, 65 (2011) 962.
20. M. Figlarz, F. Fievet and J. Lagier, US Patent No. 4539041, 1985.
21. G. Janssena, E. Sittersa and A. Pfrang, *J. Power Sources*, 191 (2009) 501.
22. E.A. Ticianelli, C.R. Derouin, A. Redondo and S. Srinivasan, *J. Electrochem. Soc.* 135 (1988) 2209.
23. N. Gavrilov, M. Vujković, I. Pašti, G. Ćirić-Marjanović and S. Mentus, *Electrochim. Acta*, 56 (2011) 9197.
24. T. Maiyalagan and B. Viswanathan, *Mater. Chem. Phys.*, 93 (2005) 291.
25. G. Socrates, *Infrared and Raman Characteristic Group Frequencies*, Wiley, New York (2001).
26. L. Bellamy, *The infra-red spectra of complex molecules,* John Wiley & Sons Inc., New York (1956).
27. Y. Shao, G. Yin, J. Wang, Y. Gao and P. Shi, *J. Power Sources* 161 (2006) 47.
28. A. Taylor, M. Michel, R. Sekol, J. Kizuka, N. Kotov and L. Thompson, *Adv. Funct. Mater.*, 18 (2008) 3003.
29. Y. Zhou, K. Neyerlin, T. Olson, S. Pylypenko, J. Bult, H. Dinh, T. Gennett, Z. Shao and R. O'Hayre, *Energy Environ. Sci.*, 3 (2010) 1437.